Microwave Dielectric and Mechanical Behavior of Foams from Polystyrene and Poly(methyl methacrylate) Blends

TAPAN K. CHAKI*, *Radar and Communication Centre Indian Institute of Technology Kharagpur - 721302, India* and P. C. BANDYOPADHYAY, *Materials Science Centre, Indian Institute of Technology, Kharagpur - 721302, India*

Synopsis

Foams have been generated from blends of polystyrene and poly(methyl methacrylate) under identical conditions of solvent–nonsolvent ratio, impregnation time, and heating period. Scanning electron micrographs of copper-coated fractured surfaces of the samples reveal a distinct transition in their structures from a more or less homogeneous cell-size distribution with prominent grain boundaries to complete lack of foaming and cellularity through random dispersions of spherical poly(methyl methacrylate) inclusions in polystyrene-foam matrix. Dielectric measurements have been made on test specimens at 9.375 GHz X-band microwave frequency by the method of Smith and Hippel modified by Dakin and Works. Percent porosity is the least at 20 wt% of polystyrene while foam density linearly decreases with percent porosity. Dielectric constant is linear in foam density on direct and semilog scales (passing through unity and zero, respectively), in blend composition and also in percent porosity. Dielectric constant increases with increase of foam density or weight percent of polymethylmethacrylate and decreases with increase of percent porosity. The dielectric constant is, however, nonlinear in volume fraction of polystyrene on both direct and semilog scales, obeying Weiner's inequalities. The logarithmic law of Lichtenecker and Rother with an empirical factor 0.8276 in the index fits the data best. Specific polarization is minimal at 60 wt% of polymethyl methacrylate. The calculated Bottcher-Bruggleman plot based on the interacting spherical particle model is found to be of limited applicability. This is explained on the basis of long-range intra- and intermolecular dipole–dipole interactions. The pattern of the change of dielectric loss tangent (tan δ), lying in the range 0.150–0.045 and attaining a minimum at 20 wt% polystyrene, has similarly been explained in terms of α and β relaxations due to conformational rearrangements and steric hindrances of rotations. The compressive strength measured as a function of composition shows that the reinforcement depends on an optimization between the degree of cellularity and packing.

INTRODUCTION

Plastic cellular materials find various purposes. This is because of their low densities, high strength-to-weight ratio, good dimensional stability through appropriate resilience and hardness, nonreactivity to air, moisture, and radiations, and excellent thermal, electrical, and dielectric properties.

Electrical properties of foamed polystyrene have recently been studied in the X-band microwave region[1] at 9.375 GHz. The present paper embodies the results of investigation on the effect of addition of a polar polymer to a nonpolar one while being expanded into foams. Dielectric constants and

* To whom correspondence should be addressed.

Journal of Applied Polymer Science, Vol. 32, 3551–3564 (1986)
 CCC 0021-8995/86/023551-14$04.00

dielectric losses of foams made from blends of polystyrene (PS) and poly(methyl methacrylate) (PMMA) have been measured at a microwave frequency. Their compressive and flexural strengths have also been determined as function of composition.

EXPERIMENTAL

Materials

Materials of the following specifications were used.

(a) Styron 666, a transparent general-purpose formulation of amorphous polystyrene manufactured by Polychem Ltd., under a license from Dow Chemicals, USA (sp. gr. 1.04, Vicat softening point 99°C, sp. heat 0.3 cal/g/°C, coefficient of thermal expansion 6×10^{-5}/°C, tensile strength 365 kg/cm^2, and Izod impact strength 1.1 kg.

(b) Poly(methyl methacrylate) of high-molecular weight (procured from BDH Chemicals Ltd., Poole, England) of melt viscosity of 3.25 kilopoise (under a shear rate of 1120 s^{-1} at 240°C), and melting point 240°C.

(c) Toluene (BDH-Analar grade) used as a solvent for both polystyrene and poly(methyl methacrylatete) (boiling range 110-111°C, and weight per mL at 20°C 0.863–0.866 g), and diethyl ether (SD's LR grade) used as a nonsolvent for the polymers (boiling range 34-36°C and wt/mL. at 20°C 0.713–0.717 g).

Preparation of Blends

Mixtures of definite percentage by weight of PS and PMMA were taken and separately dissolved in Analar-grade toluene. It is found that PS completely dissolves in toluene whereas PMMA is partially soluble. Then each of the solutions were added dropwise to Analar-grade methanol in different beakers with vigorous stirring. A white coprecipitate of PS and PMMA was found collected at the bottom of the beaker, which was then filtered out. The residue in each case was a rubberlike mass and it was torn into pieces. This was then dried in a vacuum oven at 70°C for 48 h. The dry white masses are blends of PS and PMMA.

Method of Foam Generation

A known weight of the blends of PS and PMMA was taken in a beaker. These were next soaked for a fixed time in mixtures of toluene (solvent) and diethyl ether (nonsolvent) of a known volumetric composition.[1] As a result, the volatile nonsolvent was trapped within the cages of the matrices of rigid polymer chains. The soaking was done at room temperature by direct contact between the solid and the liquid interrupted by vigorous stirring. After soaking the remaining solvent-nonsolvent mixture was decanted off and the soaked polymer blends were heated in a thermostatic air oven at 90°C for a fixed time. Thus, foams from polymer blends were generated. The same procedure of foam generation was adopted with styron-666 and poly(methyl methacrylate) also.

Specimen Cutting

Test specimens for dielectric measurements were cut out and polished after random sampling from different foam structures to fit closely into waveguide.

Scanning Electron Photomicrography

Scanning electron photomicrographs of the fractured copper-coated foam samples were taken at high as well as low magnifications with ISI 60 instrument.

Density Determination

Bulk densities (in g/cm^3) of the rigid foams made from PMMA–PS blends were determined by volume and weight measurements.

Microwave Dielectric Measurement

Measurement of dielectric constant and loss of the samples were done at a single frequency of 9.375 GHz in the microwave region by the short-circuited waveguide method of Roberts and Von Hippel[2] as modified by Dakin and Works[3] for application to medium and low loss samples.[1]

Mechanical Properties

Compressive and flexural strength tests of the foam samples were performed with GDR Universal Testing Machine FU-10,000 type 147.10.

DISCUSSION

Scanning Electron Microscopy

The only report about foam generation from PMMA that appears in literature is that of a low-density foam obtained by Bartl and Bonin[4] in free radical-initiated emulsion polymerizations of methyl methacrylate using a graft copolymer of styrene and ethylene oxide as a stabilizer. Microscopic examinations of the said PMMA foam were suggestive of cell walls consisting of agglomerates of solid beads of PMMA of an approximate diameter of a few microns (μm). The mechanical strength of the foam was also found to be much lower than that of a regular polystyrene foam. In the present study, blends of PMMA and polystyrene of varying compositions have been expanded under identical conditions of heating period, impregnation time and solvent–nonsolvent ratio.

The following features are exhibited by scanning electron photomicrographs of fractured surfaces of the foam samples. Figure 1 for foam from pure PS shows a uniform appearance of PS cells with distinct grain boundaries and homogeneous cell-size distribution. The size of the cells developed is approximately of 1 μm diameter, though in some portions of the cellular structure large cavities are also visible. However, when PS blended with

Fig. 1. SEM view of the foam sample from 100% PS X 3000.

20 wt% PMMA is expanded, coarser cavities or bowls are formed as seen in Figure 2, in which some spherical balls are also present, probably created by removal or spherical PMMA particles. In certain areas the unchanged PMMA spheres are encased or surrounded by a thin layer of PS. In Figure 3 for a higher percentage of PMMA (40%), details of the arrangement are more clearly seen where a finer distribution of PMMA spheres and cavities (due to cleavage) occurs in the PS matrix with incidence of macrocavities prominently reduced. Figure 4 for foam out of a PS-PMMA mixture in equal proportions by weight reveals a more uniform distribution of PMMA spheres enveloped by the PS matrix. The photograph in Figure 5 for 60% PMMA furnishes a view of a denser packing of the PMMA spheres with cellularity still existent in their PS envelopes and also the points of their attachment both on the surface and in the interior. Finally the structure as depicted in Figure 6 for pure PMMA demonstrates a complete lack of foaming and cellularity.

Evidence of some cracks and flow in the matrix is, of course, observed. An optical microscopy of the PMMA powder used in the blends also indicated a similar spherical structure. Hence, the scanning electron microscopy of the foam samples prepared supports the findings of Bartl and Bonin[4]

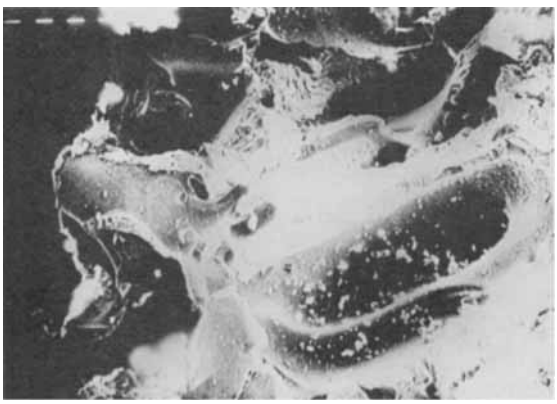

Fig. 2. SEM view of the foam sample from 80% PS and 20% PMMA X32.

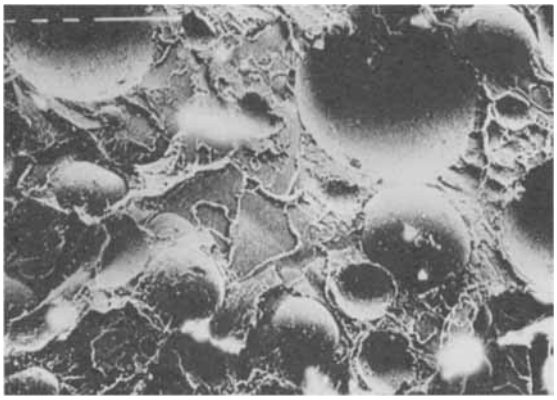

Fig. 3. SEM view of the foam sample from 60% PS and 40% PMMA X32.

that PMMA is not properly foamable, on the other hand, the foams generated here from PS-PMMA blends are nothing but compact PS foam matrices with spherical PMMA inclusions.

Percent Porosity

Though the porosity content of a rigid cellular material is usually determined by either air-compression pycnometry of differential manometry based on the work of Remington and Pariser,[5] the rough % porosity of the samples has here been calculated by a much simpler method using the relation

$$\% \text{ Porosity (p\%)} = \frac{100}{V}\left[V - \left\{\frac{x_1 m}{d_1} + \frac{(1-x_1)m}{d_2}\right\}\right]$$

where V is sample volume, x_1 the wt fraction of PS in the sample, m the sample mass and d_1 and d_2 the densities of PS and PMMA, respectively. It is found that while the foam density decreases linearly with % porosity

Fig. 4. SEM view of the foam sample from 50% PS and 50% PMMA X32.

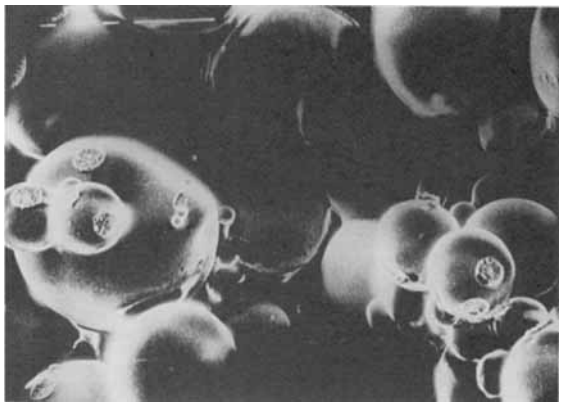

Fig. 5. SEM view of the foam sample from 40% PS and 60% PMMA X120.

(Fig. 7), the % porosity vs. composition plot (Fig. 8) shows a minimum at about 80% PMMA, corroborating the scanning electron photomicrographic evidence of a gradual fall of cellularity as the percentage of PMMA is increased.

Dielectric behavior

Dielectric constants (ϵ') of the foams under investigation exhibit a more or less linear type of relationship with their foam densities (D^*) on ordinary as well a semilog scales as shown in Figure 9. As expected, the extrapolated ϵ' for a foam of zero density, which is predominantly air, is unity. Random composite dielectrics are known to obey Wiener's inequalities[6]

$$\frac{1}{\sum_{i=1}^{m} \frac{v_i}{\epsilon_i'}} \leqslant \epsilon^* \leqslant \sum_{i=1}^{m} v_i \epsilon_i'$$

where v_i is the volume fraction of a component i in a statistical mixture of m number of components and ϵ_i' and ϵ^* are, respectively, the dielectric

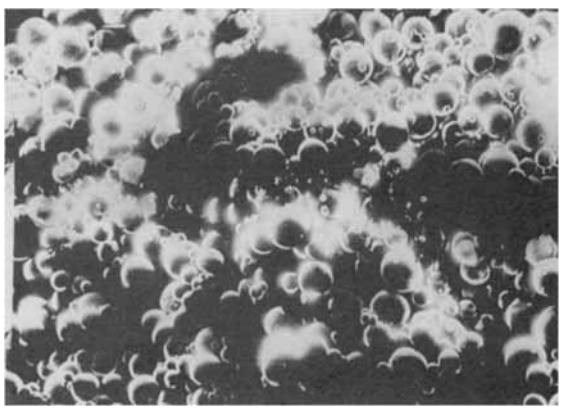

Fig. 6. SEM view of the foam sample from 100% PMMA X780.

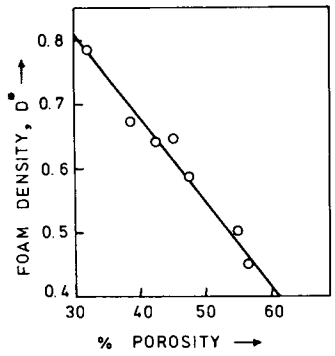

Fig. 7. Change in percent porosity with foam density of blends.

constants of pure i and the composite. On calculation of the effective ϵ' of the foams is found to lie between the specified limits. The Wiener's deviation is also quite fairly illustrated in the case by the nonlinear dependence of ϵ' on volume fraction of PS (calculated from the relation $v_1 = \frac{x_1 m}{d_1 V}$) both on ordinary and semilog scales, as shown in Figure 10. ϵ' is, however, linear both in blend composition and % porosity (Figs. 11 and 12). The logarithmic law of Lichtenecker and Rother[7] proven especially applicable to foams and porous plastics[8] is given by $\epsilon'_{\text{foam}} = \epsilon_0 D^*/D$, where ϵ_0 and D are, respectively, the dielectric constant and density of the unfoamed material. Since the foam density divided by compact density is equal to volume fraction v of solid in the foam, the above relation with D^*/D substituted for by v would apply only to foams of single systems. Hence, in the case of foams from blends as here, the products $(\frac{\log \epsilon_0}{D})\ D^*$ which are actually equal to log ϵ' can be calculated for each composition using the simple law of physical mixtures namely, $\epsilon_0 = \epsilon'_1 x_1 + \epsilon'_2 (1-x_1)$ and $D = d_1 x_1 + d_2(1-x_1)$ and then plotted against D^*. The slope of a calculated plot (Fig. 13) is 0.6137 cm^3/g as against the experimental value of 0.5079 cm^3/g, indicating again a departure from ideality. Hence, the experimental ϵ' of these foams may be represented by

$$\epsilon' = \epsilon_0 f \cdot D^*/D \quad ,$$

where $f = 0.5079/0.6137 = 0.8276$.

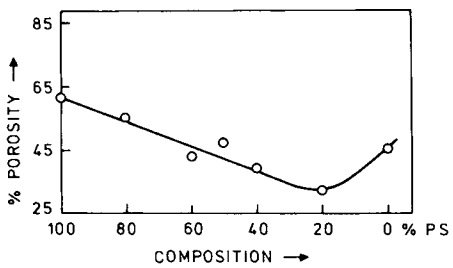

Fig. 8. Change in percent porosity with blend composition.

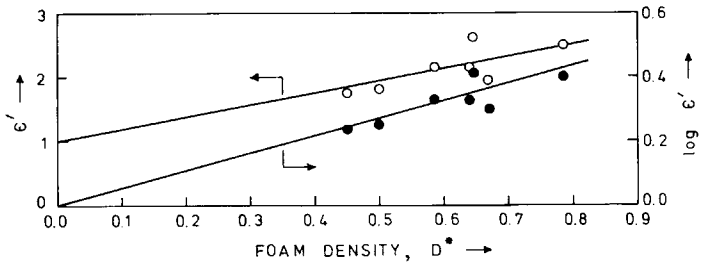

Fig. 9. Effect of foam density of PS-PMMA blend foams on ϵ' and $\log\epsilon'$.

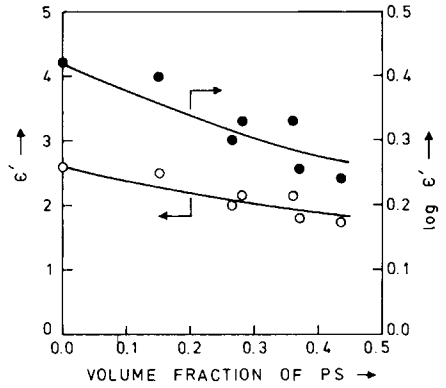

Fig. 10. Effect of volume fraction of PS in PS-PMMA blend foams on ϵ' and $\log\epsilon'$.

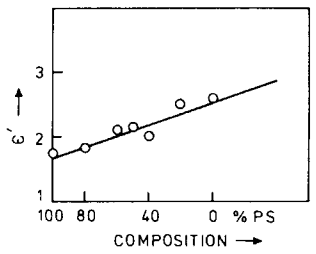

Fig. 11. Variation of dielectric constant with the change of composition in the blend foams.

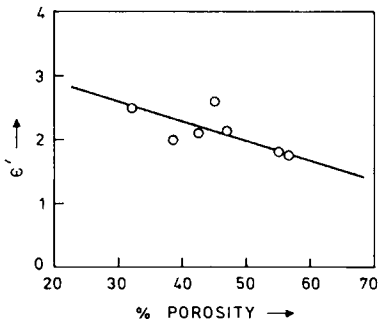

Fig. 12. Variation of dielectric constant with the change of percent porosity in the blend foams.

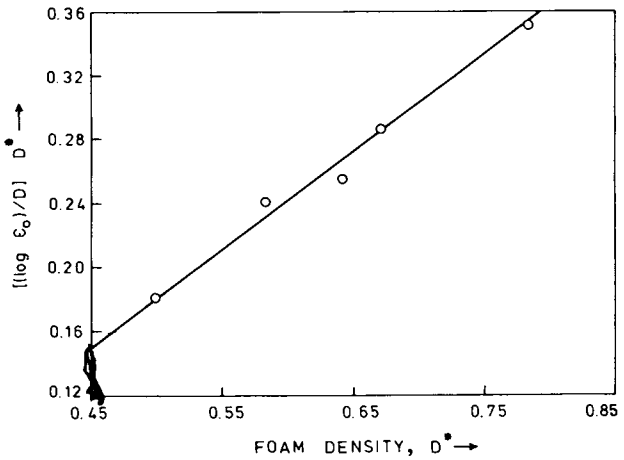

Fig. 13. Plot of $[(\log \epsilon_0)/D]D^*$ vs. foam density in the blend foams.

This behavior may be explained as follows. The blend foams, being systems of polar spheroids of PMMA sparsely and heterogeneously dispersed in the medium of a nonpolar foam matrix of PS. In such a situation, the magnitude of the short-range intra-and intermolecular dipole–dipole interaction is lessened and $(\overline{\mu^2}/N_p)^{1/2}$, the root mean square dipole moment per repeating monomer unit of the comparatively stiff PMMA chain, is increased with a corresponding increase in its ϵ_0. It may be recalled that the value of $(\overline{\mu^2}/N_p)^{1/2}$ for atactic PMMA in toluene at 30-90°C is 1.30–1.41 Debye, while μ_0, the dipole moment of methyl methacrylate monomer in benzene, is 1.60 Debye.[8] $(\overline{\mu^2}/N_p)^{1/2}$ is related to μ_0 by $\overline{\mu^2} = \Phi N_p \mu_0^2$, where N_p is the degree of polymerization and Φ a constant characteristic of molecular conformation. Though Φ is found independent of N_p and the nature of the solvent, it depends moderately on temperature, varying from 0.66 to 0.78 in the mentioned range of temperature.[9] This shows that the internal motion of a PMMA chain is not only capable of being restricted by steric repulsive forces, the different molecules in a cluster are also not absolutely free from the excluded volume effect. Dielectric interaction is actually lessened here by imposition of a nonpolar environment around polar PMMA through embedding the PMMA in PS foam matrix. This causes a smaller slope of the log ϵ' vs. D^* plot. The plot of specific polarization $(\epsilon'-1)/(\epsilon'+2)$ vs. V_2, the volume fraction of PMMA (Fig. 14), which shows a minimum polarizability per unit volume at about 60 wt% PMMA, also supports the trend of this agrument. The Bottcher-Bruggleman formula[10] for dielectric constants of two-phase mixtures, based on spherical particle models,[11] which allows for all possible interactions, as given in the review by Reynolds and Hough,[12] can be rearranged into the form

$$\epsilon' = \frac{1}{4}\left[H + (H^2 + 8\,\epsilon_1'\,\epsilon_2')^{1/2}\right]$$

where

$$H = (3v_1 - 1)\,\epsilon_1' + (2 - 3v_2)\,\epsilon_2'$$

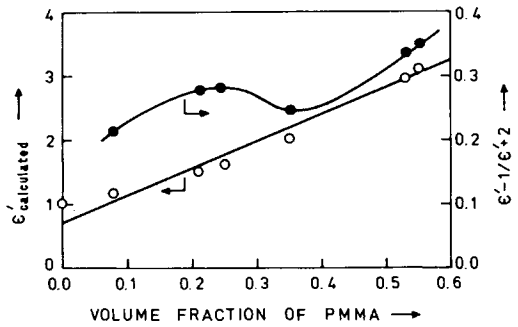

Fig. 14. Plots of ϵ'_{cal} (Bottcher-Bruggleman) and specific polarisation vs. volume fraction of PMMA in blend foams.

The expression for H has been modified here by putting it equal to $(2-3v_2)(\epsilon'_1 + \epsilon'_2) - 3p\ \epsilon'_1$ with p standing for porosity fraction. Values of ϵ' for foams have been calculated in accordance with this quadratic equation and plotted against v_2 in Figure 14. Table I shows the values of experimental ϵ' and calculated ϵ' according to Lichtenecker-Rother and Bottcher-Bruggleman relation. The linearity of this plot in contrast with the curvature observed in ϵ' vs. v_1 plot of Figure 10, therefore, suggests that the formula might be useful in representing materials where the shape and distribution of particles lead to a high degree of interaction, but in its present form it has a limited applicability especially in the case of these plastic foams, the randomly distributed spherical particles of which do not interact so considerably.

The dielectric loss tangent as shown in Figure 15 decreases with increase of PMMA content and attains a minimum value at 80 wt% PMMA, whereas it linearly increases with increase in % porosity as shown in Figure 16. It is known that Maxwell-Wagner polarization in heterogeneous dielectrics arises out of conducting contaminants, broadness in the polymers' molecular weight distribution, crystal defects (if any), structural inhomogeneity, etc., and is operative at low frequencies only. So in these foams under a microwave frequency field the entailed dielectric loss should be small and due to dipole orientational and conformational polarizations only. The observed tan δ is in the range 0.150–0.045.

Besides the primary glass rubber α transition resulting from large-scale

TABLE I
ϵ' Values Calculated and Experimental for Foams from PS-PMMA Blends

Volume fraction of PMMA in the foam	$\epsilon'_{exp.}$ (experimental)	$\epsilon'_{calc.}$ (Lichtenecker-Rother)	$\epsilon'_{calc.}$ (Bottcher-Bruggleman)
0.000	1.75	1.51	0.99
0.082	1.80	1.62	1.15
0.213	2.13	1.90	1.50
0.247	2.15	1.81	1.61
0.349	1.98	2.00	2.01
0.530	2.52	2.29	2.95
0.549	2.62	2.00	3.07

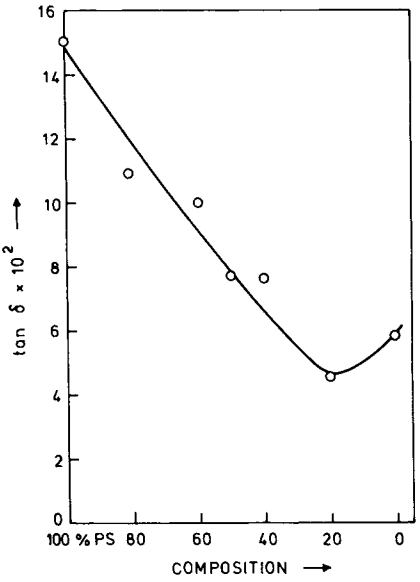

Fig. 15. Effect of composition on loss tangent in PS-PMMA blend foams.

conformational rearrangements of the polymer chain backbones which occurs in amorphous atactic PS at about 100°C and in conventional PMMA between 70° and 105°C, a secondary β relaxation is also known to be exhibited by (1) PS due to wide-angle torsional oscillations of its phenyl side groups with cooperative motion from the wriggling chains and by (2) PMMA due to hindered rotation of the ester ($-\overset{\overset{O}{\|}}{C}-OCH_3$) groups about the $-\overset{|}{\underset{|}{C}}-\overset{|}{\underset{|}{C}}-$ bonds linked to the main chain. The steric hindrance to rotation in PMMA is reported to come largely from the main chain methyl substituents of two adjacent repeat units.[13] Rotations of α-methyl groups

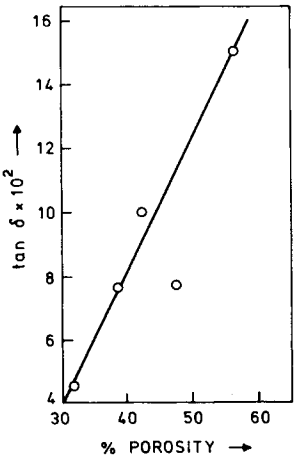

Fig. 16. Effect of percent porosity on loss tangent in blend foams.

attached directly to the main chains and of the methyl groups in the ester side chains can also take place, but they occur at low temperatures depending on the frequency of the applied sinusoidal mechanical stress. Since such rotations do not affect the net dipole moment, the corresponding γ- or δ-relaxation peaks are not observed dielectrically as proved by Sinnott.[14] However, physical mixtures of two homopolymers exhibit two relaxation regions corresponding to the α relaxations of the two polymers. Similarly, block copolymers yield two α relaxations and random copolymers yield one. This, of course, depends on compatability (i.e., on whether there are discrete regions of the pure components or a single homogeneous phase). Thus, Baer[15] found that PS-PMMA block copolymers behave as a two-phase, inhomogeneous blend giving two regions of mechanical loss maxima, though the discrete regions are of such size that they seem to be optically clear and homogeneous. On the contrary, mixtures of poly(methyl methacrylate) and polystyrene have been concluded by Hughes and Brown[16] to have contained discrete regions of the individual polymers which are so large that the characteristic properties of the individuals are retained. Mikhailov[17] studied the temperature dependence of the dielectric loss tangent of random copolymers of methyl methacrylate and styrene. He obtained only a single α peak for different compositions. But the α-loss peak, according to him, shifts to lower temperatures as the styrene proportion increases and tanδ (i.e., the magnitude of the relaxation becomes a maximum at about 60% methyl methacrylate content). It is understood that an increase in the content of nonpolar styrene lowers the relaxation magnitudes and tanδ. At the same time, at low styrene concentrations, the increase of styrene content increases the effective dipole moment of a statistical PMMA chain segment by changing the intramolecular interactions and chain conformations. The latter effect is responsible for a greater dipole orientational polarization and increase of tanδ. The present system the blend foam of PS-PMMA, however, is different from copolymer of styrene and methyl methacrylate. Unfoamable pure PMMA in which dipole-dipole interaction is quite large has here a lower tanδ than porous (heterogeneous) PS-foam (though solid atactic PS is much less lossy than atactic PMMA because of its nonpolar characteristics), but in system of PMMA domains randomly distributed in PS foam matrix, the tanδ first decreases with increasing proportion of nonpolar PS at low PS concentrations becomes a minimum at about 80% PMMA content, then goes on increasing as the foamability, heterogeneity due to greater porosity percent and dipole orientability gradually increase. The activation energy for the β-relaxation mechanism decreases with the increase in the PS content due to decreased intramolecular steric hindrance to local motion of the ester groups caused by lessened intramolecular dipole-dipole interaction. And lowered activation energy means greater relaxability and larger tanδ. The copolymers of methyl acrylate and styrene, however, behave differently.[18] First the α-loss peak moves to higher temperatures as the styrene proportion is increased. This may be due to an increase in the steric hindrance to chain backbone motions. Secondly, the location of β-loss peak is independent of the styrene concentration. This may be because the mobility of the ester groups of the acrylate units remains unaffected by styrene.

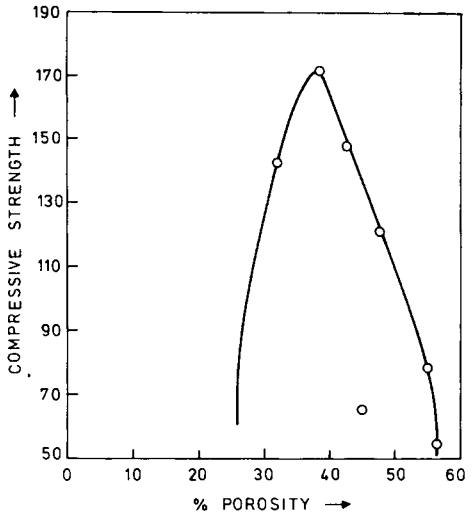

Fig. 17. Variation of compressive strength with percent porosity in blend foams.

Mechanical behavior

Ultimate compressive strength vs. percent porosity and of the same vs. blend composition presented in Figures 17 and 18 confirm that the foam made out of the blends physically becomes strongest when the composition 40% PMMA and 38.6% porosity are reached. The foams with greater percent porosity get more easily crushed by compressive forces and have consequently less strength. The strength however goes on increasing till about 40% PMMA. Hence, the reinforcement definitely depends on optimization between cellularity and degree of packing through PMMA inclusions. But the bending strength as seen from the plot of flexural strength vs. composition shown in Figure 18 reveals that the strength goes on regularly

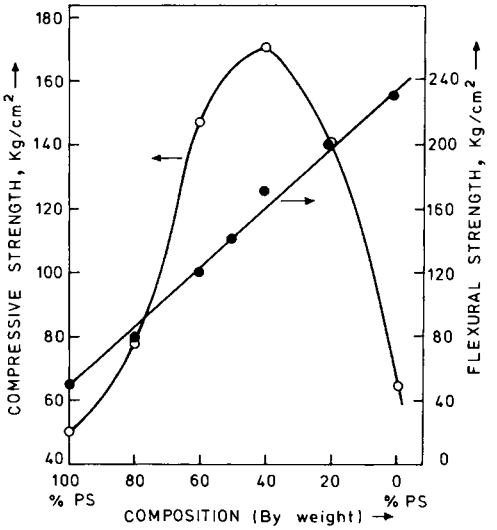

Fig. 18. Plots of flexural strength and compressive strength vs. composition of blend foams.

increasing with the increase of % PMMA content. This may be ascribed to the more rigid (i.e., to the less flexible and stiffer) nature of PMMA chains. The bending strength is, therefore, the lowest at 100% PS and the greatest at 100% PMMA apparently irrespective of the degree of cellularity of the blends. But if a close examination be made of the rate of the increase of strength with the increase of PMMA-content, it is observed that the rate of increment of strength is higher at low PMMA contents till 40% up to which only the blends are foamable. This is justified because the foams (even if rigid) are more compressible but less flexurable.

CONCLUSIONS

Rigid and mechanically strong plastic foams with excellent dielectric properties suitable for microwave region are thus possible to be generated from PS and PMMA for various Radar device constructions.

The authors wish to express their sincere thanks to Dr. D. K. Khastgir for valuable discussion.

References

1. P. C. Bandyopadhyay, T. K. Chaki, S. Srivastava, and G. S. Sanyal, *J. Polym. Eng. Sci.*, **20**(6), 441-446 (1980).
2. S. Roberts and A. Von Hippel, *J. Appl. Phys.*, **17**, 610-616 (1946).
3. T. W. Dakin and C. N. Works, *J. Appl. Phys.*, **18**, 789-796 (1947).
4. H. Bartl and W. V. Bonin (Farbenfabrik Bayer A. G., Leverkusen, Ger.) *Makromol. Chem.*, **57**, 74-95 (1962).
5. W. J. Remington, and R. Pariser, *Rubb. World*, **138**, 261 (1958).
6. O. Wiener, *Abhandl. Sachs. Ges. Wiss Math. Phys.* **K1**, 32, 509 (1912).
7. B. Tareev, *Physics of Dielectric Materials*, (translated from Russian by A. Troitsky) Mir Publishers, Moscow.
8. C. Bandyopadhyay, A. K. Banthia, and T. K. Chaki, *Die Angewandte Macromoleculare Chemie*, **120**, 61 (1984).
9. R. Salovey, *J. Polym. Sci.*, **50**, S7 (1961).
10. D. G. Crossman and J. O. Israd, *J. Phys. Appl. Phys.*, **3**, 1061 (1970).
11. L. K. H. Van Beek, *Progr. Dielectr.*, **7**, 69-114 (1967).
12. J. A. Reynolds and J. M. Hough, *Proc. Phys. Soc.*, **70B**, 769-775 (1957).
13. J. Heijboer, *Physics of Non-crystalline Solids*, North Holland, Amsterdam, 1965, p. 23.
14. K. M. Sinnott, *J. Polym. Sci.*, **42**, 3 (1960).
15. M. Baer, *J. Polym. Sci.*, **42**, 417 (1960).
16. L. J. Hughes and Brown, *J. Appl. Polym. Sci.*, **5**, 580 (1961).
17. G. P. Mikhailov, *Makromo. Chem.*, **35**, 26 (1960).
18. G. P. Mikhailov and L. V. Krasner, *Vysokomolekul. Soedin.*, **5**, 1085 (1963).

Received July 27, 1984
Accepted